Computers & Graphics 78 (2019) 54–63

Contents lists available at ScienceDirect

Computers & Graphics

journal homepage: www.elsevier.com/locate/cag

Technical Section

Exemplar-based freckle retouching and skin tone adjustment☆

Tsung-Ying Lin[a], Yu-Ting Tsai[b,*], Tsung-Shian Huang[a], Wen-Chieh Lin[a], Jung-Hong Chuang[a]

[a] Department of Computer Science, National Chiao Tung University, Taiwan
[b] Department of Computer Science and Engineering, Yuan Ze University, Taiwan

ARTICLE INFO

Article history:
Received 27 June 2018
Revised 2 November 2018
Accepted 6 November 2018
Available online 22 November 2018

Keywords:
Skin color analysis
Face beautification
Freckle retouching
Skin tone adjustment
Cosmetic transfer

ABSTRACT

This paper presents a novel system for freckle retouching and skin tone adjustment based on a set of exemplar image pairs obtained before and after cosmetic laser therapy. Our key observation is that cosmetic laser therapy relies on decomposing and adjusting melanin and hemoglobin to change skin appearance, and the reflectance properties of the two pigments can greatly influence human skin color. We thus retouch freckles and adjust skin tone in a query image by changing the densities of melanin and hemoglobin to match the variation of those in the exemplar image pairs. Based on the proposed system, we can easily and intuitively generate an output image that looks similar to the results of cosmetic laser therapy. Our system also can detect more skin flaws and define their regions more accurately than previous retouching methods.

1. Introduction

It is the nature of human beings to pursue beauty. During the last decade, researchers have proposed many freckle retouching and skin tone adjustment methods to beautify digital facial images [1–4]. There are also commercial retouching and tone adjustment smart phone applications, for example, BeautyPlus [5] and Visage Lab (http://makeup.pho.to/), and many photo editing tools for removing blemishes in an image, such as the spot healing brush in Adobe Photoshop. To the best of our knowledge, all of these software programs adjust the desired effects according to some global parameters and cannot take advantage of various skin attributes in different images. Moreover, their beautified results usually contain many artifacts, such as over-smoothing and excessive skin tone adjustment.

In this paper, we argue that the biological response of skin pigments after cosmetic laser therapy can be employed for visually pleasant retouching and tone adjustment effects, and propose a novel corresponding system based on a set of exemplar image pairs obtained before and after laser therapy. Our key observation is that cosmetic laser therapy relies on decomposing and adjusting melanin in epidermis and hemoglobin in dermis to change skin appearance, since the reflectance properties of the two pigments have a significant impact on human skin color [6]. It is reasonable to assume that similar retouching and tone adjustment effects result from similar skin attributes, and changing the freckle/skin color in a query image can be achieved by matching the densities of melanin and hemoglobin to those of exemplar image pairs from cosmetic laser therapy.

For freckle retouching, we first locate freckle regions in the query image and extract the color basis and quantities of melanin and hemoglobin for each region based on linear factor models. Then, freckle images that show the decreases in the quantities of melanin and hemoglobin after laser treatments are obtained from the exemplar images. They will appropriately guide how to eliminate the two pigments in the freckle regions. For skin tone adjustment, we model the densities of melanin and hemoglobin as Gaussian distributions and change skin color in the query image by transferring their means and standard deviations from the exemplar image pairs.

In summary, this paper makes the following contributions:

- Develop a convenient system that beautifies facial images based on the exemplars of cosmetic laser therapy.
- Combine skin color analysis and effect transfer methods for exemplar-based freckle retouching and skin tone adjustment.
- Propose an accurate hybrid detection approach for detecting freckle regions.

Note that our goal is to generate beautified facial images that look similar to the results of cosmetic laser therapy, but not to faithfully simulate the effects of laser therapy. The latter should be physiologically validated and may need a large database that contains the exemplars of numerous people. Different laser de-

☆ This article was recommended for publication by M. Glencross.

* Corresponding author.
E-mail addresses: hieicis91@hotmail.com (Y.-T. Tsai), csie9624@gmail.com (T.-S. Huang), wclin@cs.nctu.edu.tw (W.-C. Lin), jhchuang@cs.nctu.edu.tw (J.-H. Chuang).

https://doi.org/10.1016/j.cag.2018.11.002
0097-8493/

vices also have various retouching and tone adjustment effects for the same person. It is difficult to collect a large set of such diverse combinations of exemplars for experimentation and validation. Nevertheless, our results demonstrate that a small exemplar database is still effective for face/skin beautification.

2. Related work

2.1. Skin color analysis and simulation

To accurately model skin appearance and composition is important for photorealistic rendering in computer graphics and human recognition/detection in computer vision. It has been comprehensively studied in various scientific fields. Nakai et al. [7] captured the spectral reflectance data of skin in vivo and reported that skin color is mostly determined by the wavelength-dependent scattering and absorption characteristics of melanin, hemoglobin, and carotene. In [8] and [9], independent component analysis with shading removal was applied to extract principal chromatic components of skin from a single image. The authors demonstrated that the spatial variation of skin color can be faithfully represented and synthesized by two independent pigments, namely melanin and hemoglobin. In [10], human skin was considered as a multi-layered structure consisting of stratum corneum, epidermis, papillary dermis, and reticular dermis. By computing light transport through this multi-layered structure using the Kubelka–Munk theory, it was shown that all normal skin colors lie on a simple surface patch in a tristimulus color space. Angelopoulo et al. [11] employed a spectrograph to measure the bidirectional reflectance distribution function of skin over the entire visible spectrum for people of different ages, genders, and races. Readers may further refer to [6] for a comprehensive survey on skin appearance modeling.

Moreover, there are many papers that model skin color from a biophysical point of view. Donner and Jensen [12] introduced a multi-layered model of human skin to particularly account for efficient light diffusion in skin layers and multiple scattering between different layers. Based on this model, they further proposed a realistic skin shading method that relies on the amount of oil, melanin, and hemoglobin in skin [13]. Jimenez et at. [14] simulated dynamic skin appearance by measuring the distributions of melanin and hemoglobin in vivo for different facial expressions and conditions. Iglesias Guitián et al. [15] presented a biophysically-based model that simulates skin aging from the changes in the skin structure and the concentrations of chromophores, such as melanin, hemoglobin, bilirubin, carotene, and water. Chen et al. [16] considered the particle nature and distribution patterns of melanosomes to account for hyperspectral surface and subsurface scattering effects of skin appearance. They particularly modeled the hyperspectral responses of human skin to realistically render face/skin images under ultraviolet, visible, and infrared light.

In this paper, we apply the skin color analytics in [9] to obtain the color basis and quantities of melanin and hemoglobin in the query image and exemplar image pairs. Unlike previous work, the extracted information is further employed for freckle retouching and skin tone adjustment, not just for skin color synthesis after alcohol consumption, tanning, or de-aging [9].

2.2. Face/Skin beautification

Human face/skin beautification in digital images and videos has caught a lot of attention during recent decades. It is not only a challenging research problem but also an interesting and popular application of image processing. Arakawa [1] proposed to beautify facial skin using various nonlinear ϵ-filters, one of which even can be easily realized by simple hardware in multimedia systems. Leyvand et al. [17] enhanced the aesthetic appeal of human faces based on a database with attractiveness ratings. The original facial features thus can be effectively mapped to similar ones in the database with a higher rating for beautification. Lipowezky and Cahen presented an automatic freckle detection and retouching technique [3]. They detected freckles based on the blue component and saturation of each pixel, and replaced freckles with surrounding non-freckled skin regions. Nevertheless, their approach cannot find skin flaws other than freckles. By contrast, our method can detect more skin flaws, including both freckles and red patches, define their regions more accurately, and exploit real-world exemplars of cosmetic laser therapy for retouching.

Recently, Xu et al. [18] adopted bilateral filtering to remove flaws and wrinkles on the face for subsequent makeup transfer from exemplar images. Batool and Chellappa [2] developed a constrained texture synthesis algorithm to retouch facial wrinkles/imperfections with minimum user interaction. Liang et al. [19] presented an adaptive region-aware method to generate lighting, smoothness, and color masks for a facial image. Using these masks, facial beautification can be performed interactively by users or automatically by computers to achieve various skin enhancements. Liu et al. [4] employed a dual sparse coding approach to jointly solve facial hole-filling and beautification problems altogether by simultaneously matching the result to the desired target face and increasing its proximity to a set of beautiful faces. Other than images, Zhao et al. [20] designed a beautification framework for facial videos. They synthesized and tracked 3D face models for the person in an input video, so that wrinkles, freckles, and unwanted blemishes on the face can be effectively removed.

In general, previous methods have relied on image filtering/inpainting or machine learning techniques for face/skin beautification. Nevertheless, we address this problem from a biophysical point of view by analyzing and exploiting the biological response of skin pigments after cosmetic laser therapy, while focusing on freckle retouching and skin tone adjustment.

2.3. Color/Cosmetic transfer

The proposed freckle retouching and skin tone adjustment methods are conceptually similar to color transfer, which brings the color style of an image to another. Reinhard et al. [21] transferred the means and standard deviations of pixel colors in the $l\alpha\beta$ space to provide a simple but effective color correction technique. Hertzmann et al. [22] proposed to learn how pixel colors are *filtered* between two source images. The learned relationship was then utilized to *filter* a target image into a new one. Welsh et al. [23] employed a semi-automatic approach to colorize a grayscale image from a reference color image by transferring chromatic information of matching pixels with similar luminance and texture. Papadakis et al. [24] applied the concept of *spatiograms* to perform exemplar-based inpainting by transferring the spatial distribution of colors. Inspired by the drawing process of artists, Zhang et al. [25] decomposed an image into three components that represent the content, style, and stroke edges, respectively. Exemplar-based stylization thus can be faithfully achieved by propagating the style and stroke edges, but not the content, of an image to those of another. Bugeau et al. [26] colorized a grayscale image from exemplars through variational optimization and enforced the spatial coherency of neighbor pixels in the output image. Su et al. [27] demonstrated a robust color transfer method without color distortion, grain artifacts, and detail loss. Their method was also extended to color transfer from multiple references or high-dynamic-range images. Arbelot et al. [28] proposed a unified framework that relies on edge-aware texture descriptors to extract local textural content for color transfer and colorization.

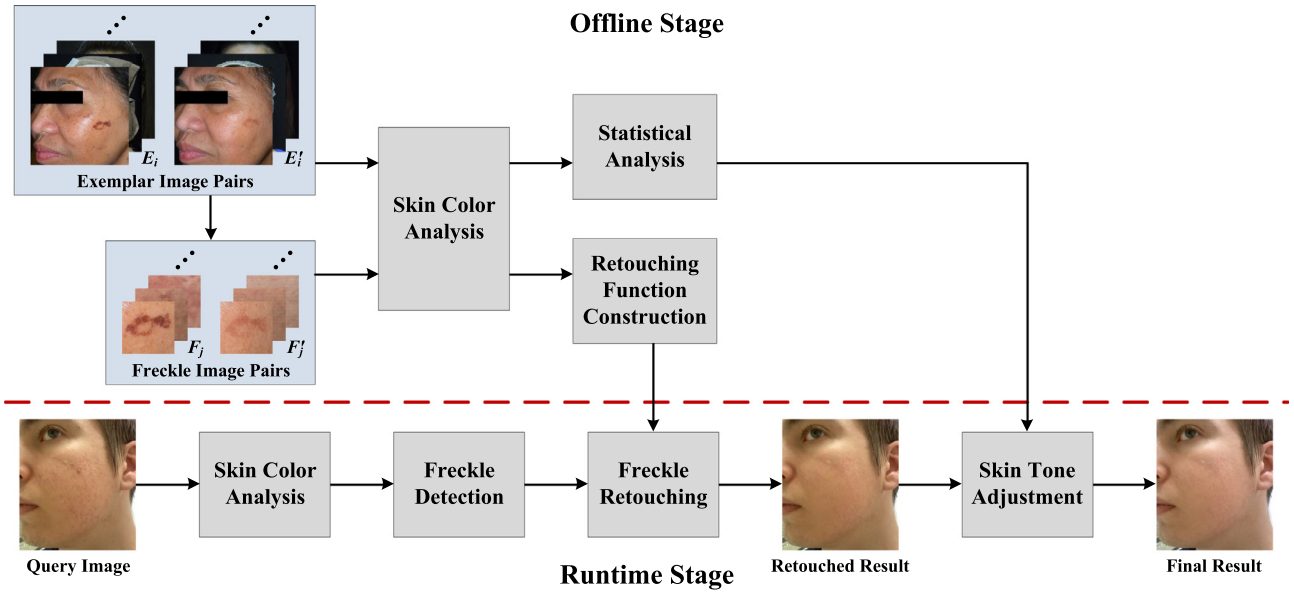

Fig. 1. Flowchart of the proposed system.

Recently, deep learning approaches have drawn a lot of attention for related problems. Iizuka et al. [29] employed convolutional neural networks to combine global and local image priors for colorization. Deshpande et al. [30] obtained multiple colorization results, whose color fields are diverse with each other but still realistic and spatially coherent, from a single grayscale image using a variational autoencoder and mixture density networks. Isola et al. [31] solved image translation problems based on conditional generative adversarial networks. The adopted networks can learn not only an image-to-image mapping but also an effective loss function for training the mapping.

In addition to color styles, transferring cosmetic effects from exemplar images has been studied over the last decade. Tong et al. [32] proposed to learn the changes in color and illumination due to makeup from *before-and-after* exemplar image pairs. To exclude transferring skin flaws in the exemplar images, skin texture and tone were also adjusted based on the extracted information by using skin color analysis. Guo and Sim [33] respectively decomposed the exemplar and subject images into the face structure, skin detail, and color layers. The makeup information of each layer thus can be separately transferred in different ways from the exemplar image to the subject one. Scherbaum et al. [34] found mappings from facial appearance to makeup from a database of exemplar facial images with and without professional makeup. An input facial image without makeup then can be transformed into a new one with the best-fit makeup in the database.

In this paper, we instead focus on transferring the freckle retouching and skin tone adjustment effects from exemplar images obtained before and after cosmetic laser therapy. Moreover, to the best of our knowledge, we are not aware of any prior work on exemplar-based skin tone adjustment.

3. System overview

The proposed system is divided into offline and runtime stages, as shown in Fig. 1. In the offline stage (Section 4), exemplar facial image pairs of different people, (E_i, E_i') for $i = 1, \ldots, N$, are collected before (E_i) and after (E_i') cosmetic laser treatments. For freckle retouching, we first generate freckle image pairs, (F_j, F_j') for $j = 1, \ldots, N'$, each of which contains the corresponding subimages of the same freckle region in an exemplar image pair (Section 4.1). After skin color analysis (Section 4.2), retouching functions are then constructed for each freckle region to represent the decreases in the quantities of melanin and hemoglobin of each pixel in F_j and F_j' (Section 4.3). As for skin tone adjustment, we model the densities of melanin and hemoglobin in E_i and E_i' as Gaussian distributions (Section 4.4), whose statistical parameters, namely means and standard deviations, will be adopted at runtime to change skin color in the query image.

In the runtime stage, we first detect freckle regions in the query image Q for freckle retouching, according to the gradient of skin color and the histograms of melanin and hemoglobin (Section 5.1). Our system then finds suitable freckle image pairs and applies their retouching functions to transfer the effects of cosmetic laser therapy (Section 5.2). For skin tone adjustment (Section 6), we also search for appropriate exemplar image pairs and employ their Gaussian distribution parameters to transfer changes in melanin and hemoglobin from exemplars to the query image.

To avoid imposing undesirable effects on non-skin regions, our system requires the user to provide skin masks of each exemplar image and the query image as additional inputs. Note that these masks can be generated manually or using automatic/semi-automatic methods [3,19,33]. A comprehensive survey on skin mask generation is beyond the scope of this paper. Readers may refer to [19] and references therein. In the following sections, we assume that all skin masks are already available and implicitly applied to their corresponding images before each step of the proposed system.

4. Offline preprocessing

4.1. Freckle image generation

For freckle retouching, the local color variation of each freckle is more important than the global variation of the whole skin in an image. Nevertheless, skin appearance is considerably different between a pair of *before-and-after* exemplar images (E_i, E_i'). A person may also look different at distinct time. In our database, for example, a female participant became slimmer when taking her *after* image. It is thus difficult to precisely align E_i with E_i' for analyzing the local color variation of each freckle. To overcome this issue, we manually locate the corresponding freckle regions in E_i and E_i' by

visual inspection, and crop E_i and E_i' to generate the freckle image pairs, each of which contains the corresponding subimages of the same freckle region. The top left corner of Fig. 1 shows an example of the exemplar and freckle image pairs. Note that we currently do not perform registration on freckle image pairs to account for misalignment between E_i and E_i'. This may lead to biased density estimation of melanin and hemoglobin in skin color analysis and further influence retouching functions. Nevertheless, we did not observe any noticeable artifacts that result from this issue in our experiments, since the *after* image of each participant was taken with a neutral expression from a similar viewpoint of his/her *before* image, and freckle image pairs were carefully cropped by hand. Under this controlled condition, both misalignment and biased density problems can be alleviated. If needed, non-rigid image registration methods [35,36] can be additionally employed on each freckle image pair to improve the quality of estimated quantities of skin pigments.

4.2. Skin color analysis

According to biophysical studies [6,7], human skin color is almost dominated by the scattering and absorption characteristics of melanin and hemoglobin. Cosmetic laser therapy also relies on selective photothermolysis to decompose the two pigments for freckle retouching and skin tone adjustment. In this paper, we basically follow the method proposed by Tsumura et al. [9] to analyze skin color. For an image, surface reflection is first removed by employing the specular-diffuse separation technique based on the Ch-CV space [37]. Shading on the face is further removed using principal component analysis as in [9], and independent component analysis proposed in [8] is then applied to extract the color basis and quantities of melanin and hemoglobin for subsequent use. Tsumura et al. [9] assumed that the color vectors of melanin and hemoglobin are statistically independent and their weighted summation well approximates skin color without surface reflection and shading. By analyzing the log-space pixel colors in an image/patch using independent component analysis [8], the extracted summation weights are regarded as the quantities of melanin and hemoglobin.

4.3. Retouching function construction

The decreases in the quantities of melanin and hemoglobin after cosmetic laser therapy can serve as an important guide for freckle retouching. From each freckle image pair, for example (F_j, F_j'), we construct two retouching functions, one for melanin and the other for hemoglobin, to represent the mapping from the quantity of melanin/hemoglobin of each pixel in F_j to the eliminated quantity of melanin/hemoglobin of the corresponding pixel in F_j'. As shown in Fig. 2, a retouching function thus can be regarded as a *quantity* transfer function (like a color transfer function in visualization) whose input and output are respectively the quantity of melanin/hemoglobin and the eliminated quantity after cosmetic laser therapy. Since the obtained basis vectors of melanin and hemoglobin after skin color analysis are statistically independent, it is intuitive to process the two pigments individually. In the next paragraph, we just explain how to construct the retouching function of melanin, while that of hemoglobin can be similarly obtained.

Specifically, we apply piecewise linear regression [38] to model a retouching function as a piecewise linear curve. For a freckle image pair (F_j, F_j'), the eliminated quantity of melanin between a pixel p in F_j and its corresponding pixel p' in F_j' is computed as $\Delta M_j(p) = M_j(p) - M_j'(p')$, where $M_j(p)$ and $M_j'(p')$ denote the quantities of melanin of p and p', respectively. In the 2D space

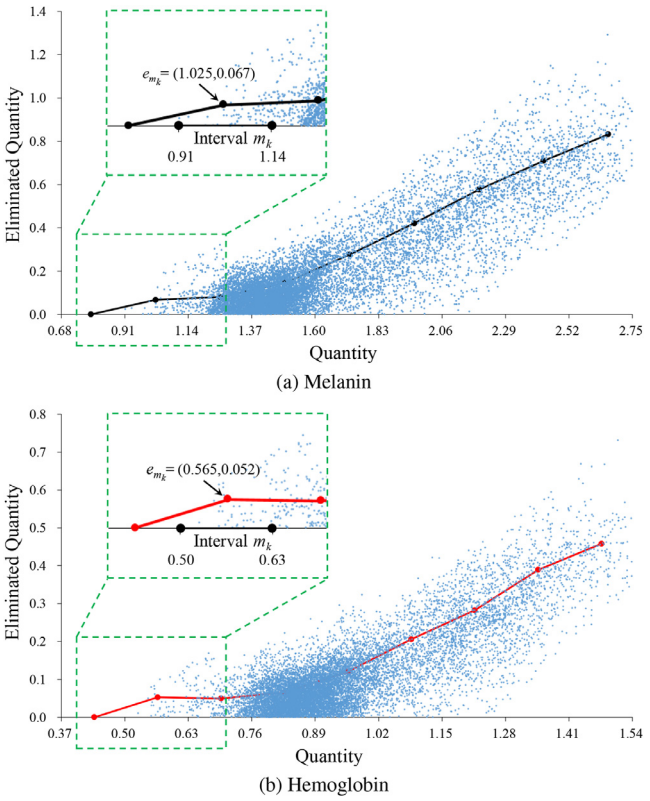

Fig. 2. Retouching functions of melanin and hemoglobin. In each subfigure, the enlarged part highlights the endpoint of an interval and its 2D coordinates.

spanned by M_j and ΔM_j, we fit a piecewise linear curve for all pixels in F_j by first dividing M_j into K uniform intervals $\{m_k\}_{k=1}^{K}$. The center of an interval m_k and the mean of ΔM_j within m_k then compose the 2D coordinates of a segment endpoint e_{m_k}, as in Fig. 2(a). The piecewise linear curve $R_j(\cdot)$, namely the retouching function of melanin for an image pair (F_j, F_j'), is finally constructed by sequentially connecting the endpoint of each interval, and can be defined as

$$R_j(M) = \begin{cases} a_1\left(M - e_{m_1}^{(x)}\right) + e_{m_1}^{(y)} & \text{for } e_{m_1}^{(x)} \le M < e_{m_2}^{(x)}, \\ \vdots & \vdots \\ a_{K-1}\left(M - e_{m_{K-1}}^{(x)}\right) + e_{m_{K-1}}^{(y)} & \text{for } e_{m_{K-1}}^{(x)} \le M < e_{m_K}^{(x)}, \end{cases} \quad (1)$$

where M denotes the input melanin quantity, a_k is the slope of the k-th segment, and $e_{m_k}^{(x)}$ and $e_{m_k}^{(y)}$ respectively specify the x and y coordinates of the segment endpoint e_{m_k}. Note that each segment is actually a line and adjacent ones are connected at a segment endpoint, for instance the $(k-1)$th and kth segments at e_{m_k}. In addition, one can apply more sophisticated approaches to represent retouching functions, such as nonlinear regression analysis. Nevertheless, we have found that the proposed simple method is adequate to generate convincing results from our experiments.

4.4. Statistical analysis for skin tone adjustment

We only focus on the global perception of skin tone adjustment to avoid transferring white patches from exemplars. Our system thus relies on the global statistics of melanin and hemoglobin in each exemplar image pair to achieve this goal. The densities of the two pigments are simply modeled as Gaussian distributions, whose statistical parameters, namely means and standard deviations, are computed offline and will be employed for tone adjustment in the runtime stage.

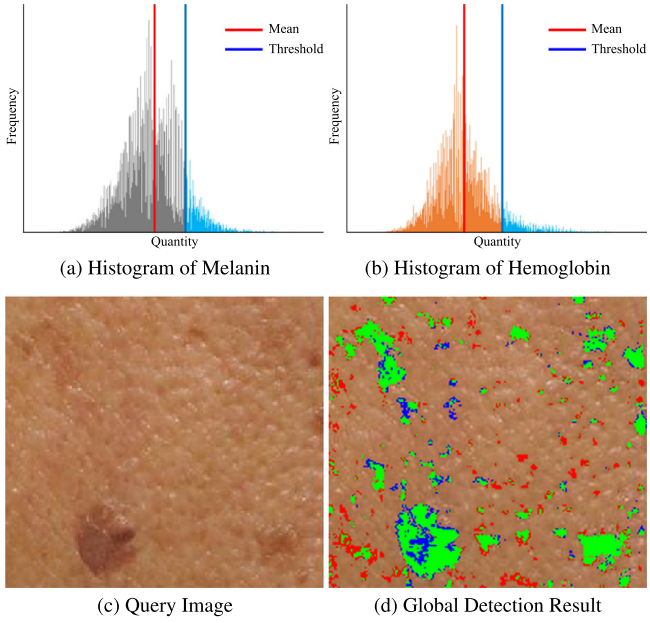

Fig. 3. Global detection of freckles and red patches by automatically thresholding on the quantity histograms of melanin and hemoglobin in the query image. The threshold is determined by the mean and standard deviation of melanin/hemoglobin. The subfigure (d) shows detected freckles (in blue), red patches (in red), and both (in green). (For interpretation of the references to color in this figure legend, the reader is referred to the web version of this article.)

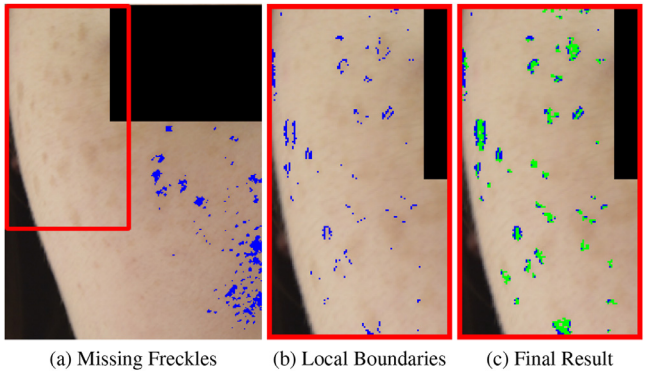

Fig. 4. Local detection of freckles. (a) The proposed global scheme can detect most freckles (highlighted in blue), but misses those inside the red rectangle. (b) Local detection instead can find boundaries of the missing freckles. (c) The final result of local detection after region growing. Pixels found by region growing are highlighted in green. (For interpretation of the references to color in this figure legend, the reader is referred to the web version of this article.)

5. Freckle detection and retouching

5.1. Freckle detection

Although it is known that the quantities of melanin and hemoglobin are high in the regions of freckles and red patches, automatically and accurately detecting them in the query image Q is not trivial. In this paper, we propose a hybrid method that combines global and local detection schemes. The global scheme is capable of locating most freckles and red patches, while the local one is suitable for detecting them in highlighted/shadowed regions. Note that lips and ears in Q are excluded from the detection process, since the hemoglobin of lips is usually higher than that of human skin. The self-shadowing effect of ears also leads to some detection problems. In the following paragraphs, we just explain how to detect freckles based on melanin. Red patches can be similarly located based on hemoglobin instead.

5.1.1. Global detection

As shown in Fig. 3, a simple but efficient technique is applied to detect most freckle regions. By thresholding on the quantity histogram of melanin in Q, a pixel with melanin above the threshold is considered as a freckle pixel. Freckle regions then can be obtained by computing the 8-connected components of freckle pixels. Note that the threshold value is determined by $\overline{M}_Q + \alpha \cdot \sigma_Q$, where $\overline{M}_Q$ and σ_Q respectively denote the mean and the standard deviation of melanin in Q, and α is a user-specified constant (within [0.8,1.2] in our experiments). Although there may be some pixels that are misclassified as freckles after global detection and then retouched, the changes in their color values are small in practice, since the skin pigment quantities of corresponding pixels in the freckle image pairs also do not vary a lot. It is not a significant issue to misclassify non-freckle pixels as freckle ones, but would be a serious problem with missing freckles.

5.1.2. Local detection

In our experience, even if the effect of shading was removed during skin color analysis, the proposed global scheme usually cannot detect freckles in highlighted/shadowed regions. Furthermore, even after removing all kinds of pigmentation, the skin color of a human is still not smooth. It is thus difficult to employ one threshold on the quantity histogram of melanin in the whole image to detect all freckles on the face. Fig. 4(a) demonstrates an example of missing freckles after global detection.

To solve this issue, we combine local statistics of the quantity histogram and gradient for detecting missing freckles. After global detection, the query image is uniformly divided into grid cells, whose quantity histogram and gradient of melanin are separately computed and thresholded. A pixel that exceeds both the local quantity and gradient thresholds is regarded as locating on the boundaries of a freckle region, such as blue pixels in Fig. 4(b). Note that while the gradient threshold is specified by the user, the quantity threshold is determined similarly to the global scheme but instead based on the mean and standard deviation of melanin in a cell. Currently, we only consider local statistics of individual cells and ignore those of adjacent cells. Although this may induce inappropriate statistical estimation for pixels close to cell boundaries, no significant artifacts were found in our experiments.

After thresholding, a region growing method is then applied to refine freckle regions. We assume that the melanin of a boundary pixel is somewhat less than that of an interior pixel. Therefore, a pixel 8-adjacent to an existing freckle region is added to the region if its melanin is more than the mean of region boundaries. The above growing step is repeated until no regions are further expanded. Finally, the result of local detection is obtained by computing the 8-connected components of existing freckle regions, as in Fig. 4(c).

The cell size for local detection depends on the query image and was empirically determined in our experiments. A large cell size would generate a similar result to global detection (the extreme case). On the other hand, a small one accounts for local statistical variations in the query image, and tends to detect detailed freckles easily. From our experience, a cell size of 32×32 or 64×64 is typically suitable for a query image with a resolution of 1024×1024, and was employed for all experimental results in this paper unless specified. Fig. 5 further demonstrates the results of local detection with three different cell sizes. With the decrease in the cell size, more detailed freckles can be detected.

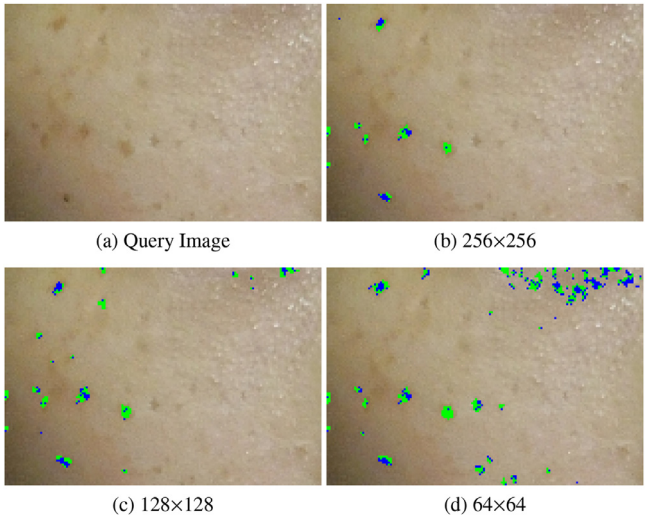

Fig. 5. Local detection of freckles with different cell sizes (shown under each subfigure). Pixels found by thresholding and region growing are highlighted in blue and green, respectively. (For interpretation of the references to color in this figure legend, the reader is referred to the web version of this article.)

5.2. Freckle retouching

We follow the concept of cosmetic laser therapy to retouch freckles and red patches by eliminating their quantities of melanin and hemoglobin, such that their color is similar to surrounding skin color. The elimination process particularly relies on linearly interpolating the retouching functions that are constructed from freckle image pairs in the offline stage (Section 4.3). The interpolated result then can be employed to reduce the melanin/hemoglobin of each pixel in a freckle region. In this subsection, we only present the proposed freckle retouching method based on melanin, while red patches can be similarly handled by eliminating hemoglobin instead.

For a detected freckle region r in the query image, we search for freckle image pairs with similar mean quantities of melanin. The similarity S_j between r and a freckle image pair (F_j, F_j') is defined as

$$S_j = \overline{M}_r - \overline{M}_{F_j}, \tag{2}$$

where $\overline{M}_r$ and $\overline{M}_{F_j}$ are the mean quantities of melanin in r and F_j, respectively. Freckle image pairs whose similarity values are less than a user-specified threshold t_r are selected for retouching freckles in r by linearly interpolating their retouching functions as

$$R\big(M_r(p)\big) = \sum\nolimits_j w_j R_j\big(M_r(p)\big), \tag{3}$$

where $M_r(p)$ is the quantity of melanin of a pixel p in r, $R(\cdot)$ and $R_j(\cdot)$ are respectively the retouching functions of melanin for r and a selected freckle image pair (F_j, F_j'), and

$$w_j = \frac{e^{-\epsilon S_j^2}}{\sum_k e^{-\epsilon S_k^2}} \tag{4}$$

is the normalized interpolation weight of $R_j(\cdot)$, with a user-specified constant ϵ (heuristically set to 16 in our experiments). We then employ the derived retouching function $R(\cdot)$ to decrease the melanin of each pixel in r. Fig. 6(a) illustrates an example of interpolating the retouching functions of melanin.

After elimination, the mean skin color in r may still be slightly different from its surroundings, as shown in Fig. 7(b). We thus further add $\overline{M}_s - \overline{M}_r$ to the melanin of each pixel in r, where $\overline{M}_s$ is the mean quantity of melanin of pixels that are 8-adjacent to r.

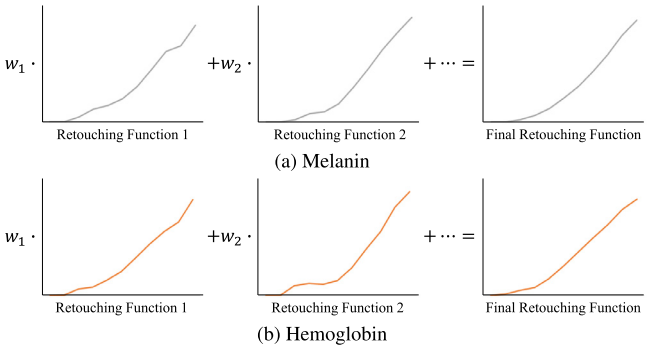

Fig. 6. Interpolating the retouching functions of melanin and hemoglobin for selected freckle image pairs. For each retouching function, the horizontal and vertical axes are the quantity and eliminated quantity of melanin/hemoglobin, respectively. The symbols w_1 and w_2 represent the interpolation weights of retouching functions.

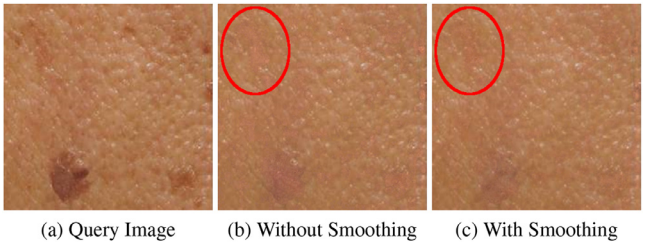

Fig. 7. Comparison of freckle retouching with and without smoothing: (b) retouching only by eliminating melanin; (b) retouching by both elimination and smoothing.

Fig. 7(c) demonstrates an example of the smoothed result (also the final result of freckle retouching).

6. Skin tone adjustment

The proposed skin tone adjustment method was inspired by color transfer [21], which changes the appearance of an image by using the global statistics of pixel colors in another image. Instead of pixel colors, we employ the means and standard deviations of melanin and hemoglobin in the exemplar image pairs, which are already precomputed in the offline stage, to adjust skin tone in the query image after freckle retouching.

We search for exemplar image pairs with similar mean quantities of melanin and hemoglobin to the query image Q. The similarity S_i' between Q and an exemplar image pair $\left(E_i, E_i'\right)$ is defined as

$$S_i' = \sqrt{\left(\overline{M}_Q - \overline{M}_{E_i}\right)^2 + \left(\overline{H}_Q - \overline{H}_{E_i}\right)^2}, \tag{5}$$

where $\overline{M}_Q$ and $\overline{M}_{E_i}$ respectively denote the mean quantities of melanin in Q and E_i, while $\overline{H}_Q$ and $\overline{H}_{E_i}$ similarly specify hemoglobin. Exemplar image pairs whose similarity values are less than a user-specified threshold t_Q are selected for skin tone adjustment. We then offset the mean of melanin/hemoglobin in Q by the difference between linearly interpolated means from selected *before-and-after* exemplar images. The standard deviation of melanin/hemoglobin in Q is also scaled by the ratio of interpolated standard deviations from selected exemplars. After that, the result of skin tone adjustment can be obtained by transforming the quantities of melanin and hemoglobin back into skin color, as shown in Fig. 8(b).

More formally, let $M_Q(p)$ be the quantity of melanin of a pixel p in Q. We adjust $M_Q(p)$ by

$$\left(M_Q(p) - \overline{M}_Q\right)\frac{\sigma_{E'}}{\sigma_E} + \overline{M}_Q + \left(\overline{M}_{E'} - \overline{M}_E\right), \tag{6}$$

(a) Before (b) After

Fig. 8. Comparison of images before and after skin tone adjustment.

with

$$\overline{M}_E = \sum_i w_i \overline{M}_{E_i}, \qquad \sigma_E = \sum_i w_i \sigma_{E_i}, \tag{7}$$

$$\overline{M}_{E'} = \sum_i w_i \overline{M}_{E'_i}, \qquad \sigma_{E'} = \sum_i w_i \sigma_{E'_i}, \tag{8}$$

where σ_{E_i} and $\sigma_{E'_i}$ are respectively the standard deviations of melanin in E_i and E'_i in a selected exemplar image pair (E_i, E'_i), and the normalized interpolation weight of (E_i, E'_i), namely w_i, is defined as Eq. (4) but instead using the similarity metric in Eq. (5).

Since we approximate melanin densities as Gaussians, Eq. (6) actually applies the Gaussian transformation (from E_i to E'_i) to the melanin densities of Q, which is similar to the transformation of an arbitrary normal into the standard normal. The first two terms in Eq. (6) adjust the standard deviation of melanin quantities in Q with respect to the standard deviation scale in E_i over E'_i. The last term instead changes the mean of melanin quantities in Q with respect to the mean offset from E_i to E'_i. Note that the quantity of hemoglobin of each pixel in Q can be similarly adjusted as Eq. (6) from the statistical parameters of hemoglobin in the selected exemplar image pairs.

7. Experiments

7.1. Results

Our exemplar database consists of 15 *before-and-after* image pairs, some of which were provided by a cosmetic clinic and the others were collected from the internet. The proposed freckle retouching and skin tone adjustment methods were tested on facial images that contain different sizes, amounts, and distributions of freckles and red patches. All the experiments were conducted on a PC with an Intel Xeon E3-1230 v2 CPU.

Fig. 9 compares the proposed freckle detection and retouching methods with [3]. In Fig. 9(e), the red patches on both sides of the girl's nose bridge cannot be detected and retouched by [3]. Shading on the face is also not well preserved in the results of [3]. By contrast, these problems do not exist in our results. For detection, the approach in [3] globally captures only freckles based on skin color values. Nevertheless, our method combines global and local schemes to improve detection accuracy and obtains both freckles and red patches by using the extracted information of melanin and hemoglobin from skin color analysis. Furthermore, since shading on the face is not considered by [3], some shadowed regions may be falsely detected as freckles and retouched. For example, note the nostrils and around the nose in Fig. 9(b) and (e).

Fig. 10 demonstrates two exemplar image pairs from cosmetic laser therapy, the results of the smart phone application BeautyPlus [5], and our results using Fig. 10(a) and (e) as query images. The error from the ground truth, namely Fig. 10(b) or (f), without surface reflection is also shown under each subfigure. Since participants in our database look very different when taking his/her *before* and *after* images, without accurate facial image alignment and

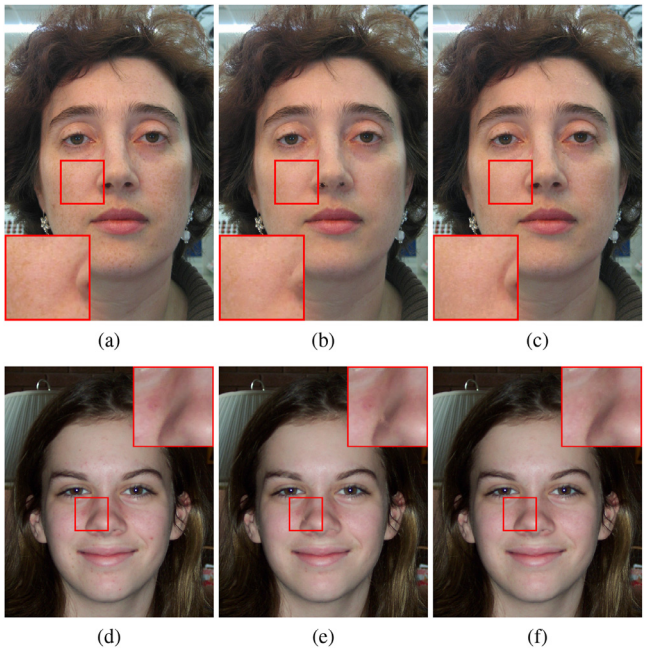

(a) (b) (c)

(d) (e) (f)

Fig. 9. Comparison of the proposed freckle retouching method and [3]: (a), (d) query images; (b), (e) results of [3]; (c), (f) our results after retouching. Subfigures (a), (b), (d), and (f) were provided by Lipowezky and Cahen from [3]. (For interpretation of the references to color in this figure, the reader is referred to the web version of this article.)

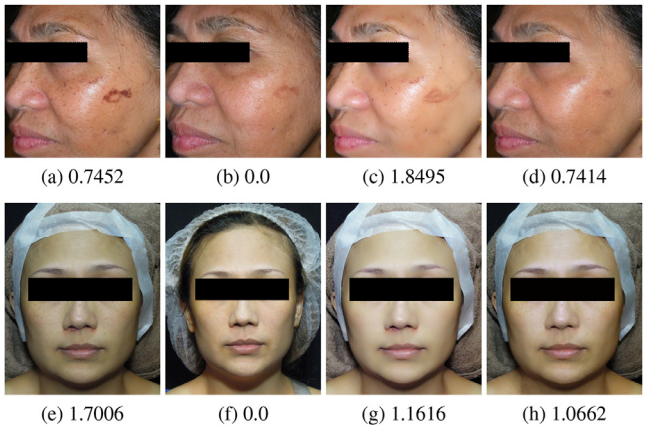

(a) 0.7452 (b) 0.0 (c) 1.8495 (d) 0.7414

(e) 1.7006 (f) 0.0 (g) 1.1616 (h) 1.0662

Fig. 10. Comparison of the proposed system, cosmetic laser therapy, and BeautyPlus [5]: (a), (e) before therapy; (b), (f) after therapy; (c), (g) results of BeautyPlus; (d) our result after retouching; (h) our result after retouching and tone adjustment. Subfigures (a) and (d) are respectively the query images for (c) and (g) using BeautyPlus as well as for (d) and (h) based on our system. Under each subfigure, its total error of skin color distributions from the ground truth, namely (b) or (f), without surface reflection is shown and a lower value is better.

warping, an incorrect error would be obtained using common image quality metrics, such as the root-mean-square error and other visible difference predictors. We instead measure the error by computing the difference of normalized skin color histograms between two images, which is defined as

$$\sum_c \sum_i \left| \frac{H_1^c(b_i)}{\sum_j H_1^c(b_j)} - \frac{H_2^c(b_i)}{\sum_j H_2^c(b_j)} \right|, \tag{9}$$

where $H_1^c(b_i)$ and $H_2^c(b_i)$ are the total number of skin pixels within a bin b_i for a color channel c in the two images, respectively. Note that we normalize the pixel number within a bin to account for different numbers of skin pixels in the two images and thus convert skin color histograms into statistical distributions. We also

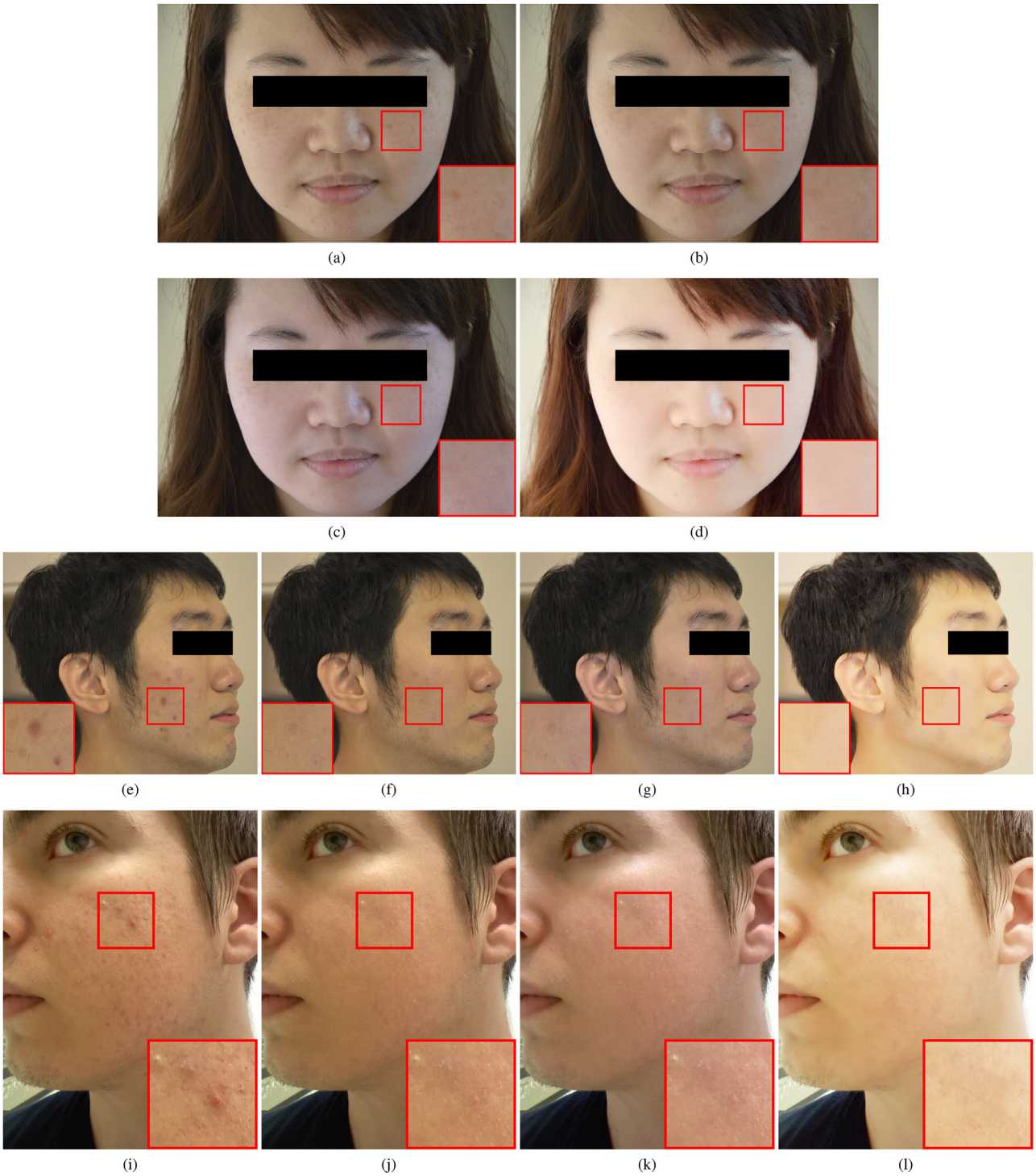

Fig. 11. Comparison of the proposed system and BeautyPlus [5]: (a), (e), (i) query images; (b), (f), (j) our results after retouching; (c), (g), (k) our results after retouching and tone adjustment; (d), (h), (l) results of BeautyPlus. (For interpretation of the references to color in this figure, the reader is referred to the web version of this article.)

compute errors in the La^*b^* color space, whose color value changes are closely and linearly related to the response of human eyes.

Due to the current small exemplar database, a large value of the constant ϵ in Eq. (4) should be adopted for effective interpolation. The differences between our results and those of laser therapy are sometimes perceptible, such as Fig. 10(b) and (d). Although this issue can be solved by collecting more *before-and-after* image pairs and using a smaller ϵ for the interpolation kernel, the retouching and tone adjustment effects in Fig. 10(d) and (h) are still more similar to laser therapy than those of BeautyPlus, in terms of skin color distributions. We believe that the proposed system could potentially serve as a base for future research directions on previewing the effects of cosmetic laser therapy.

In Fig. 11, we demonstrate the comparison of the proposed system and BeautyPlus. Although BeautyPlus is user friendly and easy to use for novices, it may over-smooth skin flaws and excessively adjust skin tone. On the contrary, our system can generate skin appearance with convincing retouching and tone adjustment effects

Table 1
Timing statistics of the proposed system.

Result	Resolution	Offline stage			Runtime stage				
		RFC[a]	SA[a]	Total	SCA[a]	FD[a]	FR[a]	STA[a]	Total
Fig. 9(c)	631 × 953	0.03s	0.96s	0.99s	0.05s	2.43s	5.49s	–	7.97s
Fig. 9(f)	828 × 993				0.07s	2.55s	3.74s	–	6.36s
Fig. 10(d)	594 × 583				0.03s	1.05s	5.65s	–	6.73s
Fig. 10(h)	1024 × 1024				0.09s	3.43s	15.7s	0.09s	19.31s
Fig. 11(c)	1200 × 800				0.08s	1.86s	5.84s	0.09s	7.87s
Fig. 11(g)	916 × 800				0.06s	2.38s	4.9s	0.06s	7.4s
Fig. 11(k)	600 × 800				0.04s	1.38s	7.48s	0.04s	8.94s

[a] RFC: retouching function construction; SA: statistical analysis; SCA: skin color analysis; FD: freckle detection; FR: freckle retouching; STA: skin tone adjustment.

by exploiting the biological response of skin pigments after cosmetic laser therapy. The original skin texture without flaws is well preserved after retouching, while the faces and skin in the tone adjustment results have the glow of health due to our *hemoglobin-aware* approach. Note that since the adopted skin analysis method [9] was verified to be an effective approximation for the quantities of melanin and hemoglobin, our approach also has such characteristic that particularly leads to retouching and tone adjustment effects similar to cosmetic laser therapy.

Table 1 additionally lists the timing statistics of the proposed system for different results. The offline stage is very efficient and fast on the CPU. In the runtime stage, all the experiments can be accomplished within 20 s. The cost of freckle retouching depends on both the image resolution and the number of freckle regions, while that of skin tone adjustment is only related to the former.

7.2. Discussions and limitations

Previous beautification methods based on filtering, inpainting, or texture synthesis, for example [2,18], often rely on local skin appearance around the flaw regions for retouching, which may fail when there are flaws almost everywhere on skin. It is also difficult for filtering/inpainting methods to adjust skin tone. As for previous data-driven beautification approaches, such as [4,19], the biophysical knowledge of skin pigments is usually ignored. Nevertheless, our method, as well as [9,14,15], shows that the densities of melanin and hemoglobin play an important role on skin appearance. Since the applied skin color analytics was proved to well approximate the quantities of melanin and hemoglobin [9], our method can further exploit the biological response of skin pigments after cosmetic laser therapy to achieve effective freckle retouching and skin tone adjustment. Moreover, it is assumed that melanin and hemoglobin have independent influence on skin color in [9], which does not hold in the real world as reported in [39]. This inappropriate assumption may lead to misinterpreted basis vectors extracted by independent component analysis and thus incorrect quantities of melanin and hemoglobin. In this case, downgraded performance of our method is expected, such as undetected freckle regions or physiologically invalid retouching and tone adjustment effects. Fortunately, we found that this is not a big issue in practice from our experiments. As shown in Fig. 10, our results still look similar to those of laser therapy in terms of skin color distributions, even if the extracted quantities of melanin and hemoglobin may be physiologically invalid at all.

Currently, we only employ a small exemplar database to test the proposed system. If the database is not large enough, some query images may not be well retouched and adjusted. Nevertheless, it is difficult to collect a large set of real-world exemplars. While clinic customers usually refuse to offer their *before-and-after* images due to privacy issues, the resolutions of exemplars collected from the internet are usually too low to provide appropriate references.

Our method relies on some user-specified parameters, such as the constant α for global freckle detection (Section 5.1.1), the gradient and quantity thresholds for local freckle detection (Section 5.1.2), as well as the similarity thresholds for freckle retouching (Section 5.2) and skin tone adjustment (Section 6). In our experiments, these parameters were empirically determined and should be fine-tuned with respect to different query images. Although it is possible to obtain parameter values using machine learning methods, it would be difficult to learn appropriate ones with our current small laser therapy database. How to solve this problem is left as our future work.

Furthermore, there may still be some skin flaws other than freckles and red patches in our retouched results. For example, the pimple at the top left of the enlarged image in Fig. 11(j) was not detected and removed by the proposed system. Nevertheless, we believe that this issue can be solved or alleviated as long as there are corresponding *before-and-after* exemplars in the database. The proposed detection method also needs to be extended to account for more types of skin flaws, which is left as our future work.

8. Conclusion

An exemplar-based system for freckle retouching and skin tone adjustment is presented in this paper. It transfers the quantities of melanin and hemoglobin from exemplar image pairs, which are obtained before and after cosmetic laser therapy, to a query image. Since the proposed system is based on exemplars from real-world retouching and tone adjustment processes, its results particularly look similar to those of cosmetic laser therapy.

In the future, we would like to investigate more on skin color analysis. The currently applied method [9] ignores advanced lighting effects, including subsurface scattering and light absorption by pigments in skin tissues. Instead, the quantities of melanin and hemoglobin may be obtained by formulating an inverse optimization problem based on the biophysically-based spectral model [40], which accounts for full light interaction with human skin. Moreover, we are also interested in detecting and retouching more types of skin flaws, such as pimples, white patches, wrinkles, ..., etc.

Acknowledgments

We would like to thank President Chin-De Chen (from the Grammy clinic) and all participants who provided us exemplar datasets. This work was supported in part by the Ministry of Science and Technology of Taiwan under Grant Numbers MOST106-2221-E-009-146-MY3 and MOST107-2221-E-155-051-MY2.

References

[1] Arakawa K. Nonlinear digital filters for beautifying facial images in multimedia systems. In: Proceedings of the IEEE ISCAS '04. 2004, p. 429–432. doi:10.1109/ISCAS.2004.1329603.

[2] Batool N, Chellappa R. Detection and inpainting of facial wrinkles using texture orientation fields and Markov random field modeling. IEEE Trans Image Process 2014;23(9):3773–88. doi:10.1109/TIP.2014.2332401.
[3] Lipowezky U, Cahen S. Automatic freckles detection and retouching. In: IEEE Convention of the electrical and electronics engineers in Israel '08. 2008, p. 142–146. doi:10.1109/EEEI.2008.4736675.
[4] Liu X, Cheung G, Zhai D, Zhao D, Sankoh H, Naito S. Joint gaze-correction and beautification of dibr-synthesized human face via dual sparse coding. In: Proceedings of the IEEE ICIP '14. 2014, p. 4697–4701. doi:10.1109/ICIP.2014.7025952.
[5] CommSource Technology. Beautyplus. 2018. http://www.beautyplus.com/.
[6] Igarashi T, Nishino K, Nayar SK. The appearance of human skin: A survey. Found. Trends Comput Graph Vis 2007;3(1):1–95. doi:10.1561/0600000013.
[7] Nakai H, Manabe Y, Inokuchi S. Simulation and analysis of spectral distributions of human skin. In: Proceedings of ICPR '98. 1998, p. 1065–1065. doi:10.1109/ICPR.1998.711875.
[8] Tsumura N, Haneishi H, Miyake Y. Independent component analysis of skin color image. J Opt Soc Am A 1999;16(9):2169–76. doi:10.1364/JOSAA.16.002169.
[9] Tsumura N, Ojima N, Sato K, Shiraishi M, Shimizu H, Nabeshima H, et al. Image-based skin color and texture analysis/synthesis by extracting hemoglobin and melanin information in the skin. ACM Trans Graph 2003;22(3):770–9. doi:10.1145/882262.882344.
[10] Cotton S, Claridge E, Hall P. A skin imaging method based on a colour formation model and its application to the diagnosis of pigmented skin lesions. In: Proceedings of the medical image understanding and analysis '99; vol. 99. 1999, p. 49–52.
[11] Angelopoulo E, Molana R, Daniilidis K. Multispectral skin color modeling. In: Proceedings of the CVPR '01; 2001. p. 635–42. doi:10.1109/CVPR.2001.991023.
[12] Donner CS, Jensen HW. Light diffusion in multi-layered translucent materials. ACM Trans Graph 2005;24(3):1032–9. doi:10.1145/1073204.1073308.
[13] Donner CS, Jensen HW. A spectral BSSRDF for shading human skin. In: Proceedings of the EGSR '06; 2006. p. 409–17. doi:10.2312/EGWR/EGSR06/409-417.
[14] Jimenez J, Scully T, Barbosa N, Donner CS, Alvarez X, Vieira T, et al. A practical appearance model for dynamic facial color. ACM Trans Graph 2010;29(6):141. doi:10.1145/1882261.1866167.
[15] Iglesias Guitián JA, Aliaga C, Jarabo A, Gutierrez D. A biophysically-based model of the optical properties of skin aging. Comput Graph Forum 2015;34(2):45–55. doi:10.1111/cgf.12540.
[16] Chen TF, Baranoski GVG, Kimmel B, Miranda E. Hyperspectral modeling of skin appearance. ACM Trans Graph 2015;34(3):31. doi:10.1145/2701416.
[17] Leyvand T, Cohen-Or D, Dror G, Lischinski D. Data-driven enhancement of facial attractiveness. ACM Trans Graph 2008;27(3). doi:10.1145/1360612.1360637.
[18] Xu L, Du Y, Zhang Y. An automatic framework for example-based virtual makeup. In: Proceedings of the IEEE ICIP '13. 2013, p. 3206–3210. doi:10.1109/ICIP.2013.6738660.
[19] Liang L, Jin L, Li X. Facial skin beautification using adaptive region-aware masks. IEEE Trans Cybern 2014;44(12):2600–12. doi:10.1109/TCYB.2014.2311033.
[20] Zhao Y, Huang X, Gao J, Tokuta AO, Zhang C, Yang R. Video face beautification. In: Proceedings of the IEEE ICME '14. 2014, p. 1–6. doi:10.1109/ICME.2014.6890211.
[21] Reinhard E, Ashikhmin M, Gooch B, Shirley P. Color transfer between images. IEEE Comput Graph Appl 2001;21(5):34–41. doi:10.1109/38.946629.
[22] Hertzmann A, Jacobs CE, Oliver N, Curless B, Salesin DH. Image analogies. In: Proceedings of the ACM SIGGRAPH '01. 2001, p. 327–340. doi:10.1145/383259.383295.
[23] Welsh T, Ashikhmin M, Mueller K. Transferring color to greyscale images. ACM Trans Graph 2002;21(3):277–80. doi:10.1145/566654.566576.
[24] Papadakis N, Bugeau A, Caselles V. Image editing with spatiograms transfer. IEEE Trans Image Process 2012;21(5):2513–22. doi:10.1109/TIP.2012.2183144.
[25] Zhang W, Cao C, Chen S, Liu J, Tang X. Style transfer via image component analysis. IEEE Trans Multimed 2013;15(7):1594–601. doi:10.1109/TMM.2013.2265675.
[26] Bugeau A, Ta V, Papadakis N. Variational exemplar-based image colorization. IEEE Trans Image Process 2014;23(1):298–307. doi:10.1109/TIP.2013.2288929.
[27] Su Z, Zeng K, Liu L, Li B, Luo X. Corruptive artifacts suppression for example-based color transfer. IEEE Trans Multimed 2014;16(4):988–99. doi:10.1109/TMM.2014.2305914.
[28] Arbelot B, Vergne R, Hurtut T, Thollot J. Local texture-based color transfer and colorization. Comput Graph 2017;62:15–27. doi:10.1016/j.cag.2016.12.005.
[29] Iizuka S, Simo-Serra E, Ishikawa H. Let there be color!: Joint end-to-end learning of global and local image priors for automatic image colorization with simultaneous classification. ACM Trans Graph 2016;35(4):110. doi:10.1145/2897824.2925974.
[30] Deshpande A, Lu J, Yeh M, Chong MJ, Forsyth DA. Learning diverse image colorization. In: Proceedings of the CVPR '17. 2017, p. 2877–2885. doi:10.1109/CVPR.2017.307.
[31] Isola P, Zhu J, Zhou T, Efros AA. Image-to-image translation with conditional adversarial networks. In: Proceedings of the CVPR '17. 2017, p. 5967–5976. doi:10.1109/CVPR.2017.632.
[32] Tong W-S, Tang C-K, Brown MS, Xu Y-Q. Example-based cosmetic transfer. In: Proceedings of the Pacific Graphics '07. 2007, p. 211–218. doi:10.1109/PG.2007.31.
[33] Guo D, Sim T. Digital face makeup by example. In: Proceedings of the CVPR '09. 2009, p. 73–79. doi:10.1109/CVPR.2009.5206833.
[34] Scherbaum K, Ritschel T, Hullin M, Thormählen T, Blanz V, Seidel H-P. Computer-suggested facial makeup. Comput Graph Forum 2011;30(2):485–92. doi:10.1111/j.1467-8659.2011.01874.x.
[35] Ma J, Zhao J, Ma Y, Tian J. Non-rigid visible and infrared face registration via regularized gaussian fields criterion. Pattern Recognit 2015a;48(3):772–84. doi:10.1016/j.patcog.2014.09.005.
[36] Ma J, Qiu W, Zhao J, Ma Y, Yuille AL, Tu Z. Robust l_2e estimation of transformation for non-rigid registration. IEEE Trans Signal Process 2015b;63(5):1115–29. doi:10.1109/TSP.2014.2388434.
[37] Yang J, Cai Z, Wen L, Lei Z, Guo G, Li SZ. A new projection space for separation of specular-diffuse reflection components in color images. In: Proceedings of the ACCV '12. 2013, p. 418–429. doi:10.1007/978-3-642-37447-0_32.
[38] McGee VE, Carleton WT. Piecewise regression. J Am Stat Assoc 1970;65(331):1109–24. doi:10.1080/01621459.1970.10481147.
[39] Stamatas GN, Zmudzka BZ, Kollias N, Beer JZ. Non-invasive measurements of skin pigmentation in situ. Pigment Cell Res 2004;17(6):618–26. doi:10.1111/j.1600-0749.2004.00204.x.
[40] Krishnaswamy A, Baranoski GV. A biophysically-based spectral model of light interaction with human skin. Comput Graph Forum 2004;23(3):331–40. doi:10.1111/j.1467-8659.2004.00764.x.